A lysine deacetylase Hos3 is targeted to the bud neck and involved in the spindle position checkpoint

Mengqiao Wang[a,b] and Ruth N. Collins[b]
[a]Program in Biochemistry, Molecular and Cell Biology and [b]Department of Molecular Medicine, Cornell University, Ithaca, NY 14853

ABSTRACT **An increasing number of cellular activities can be regulated by reversible lysine acetylation. Targeting the enzymes responsible for such posttranslational modifications is instrumental in defining their substrates and functions in vivo. Here we show that a *Saccharomyces cerevisiae* lysine deacetylase, Hos3, is asymmetrically targeted to the daughter side of the bud neck and to the daughter spindle pole body (SPB). The morphogenesis checkpoint member Hsl7 recruits Hos3 to the neck region. Cells with a defect in spindle orientation trigger Hos3 to load onto both SPBs. When associated symmetrically with both SPBs, Hos3 functions as a spindle position checkpoint (SPOC) component to inhibit mitotic exit. Neck localization of Hos3 is essential for its symmetric association with SPBs in cells with misaligned spindles. Our data suggest that Hos3 facilitates cross-talk between the morphogenesis checkpoint and the SPOC as a component of the intricate monitoring of spindle orientation after mitotic entry and before commitment to mitotic exit.**

Monitoring Editor
Daniel J. Lew
Duke University

Received: Oct 25, 2013
Revised: May 30, 2014
Accepted: Jul 16, 2014

INTRODUCTION

Acetylation of the ε-amino group of lysine residues is a posttranslational modification (PTM) catalyzed by acetyltransferases and can be reversed via the action of deacetylases. The first identified proteins with this PTM were histones, and the role of reversible lysine acetylation is best characterized on the NH2-terminal tails of histones (reviewed in Shahbazian and Grunstein, 2007). A historical consequence of the focus on histones as substrates for reversible acetylation is that the enzymes responsible for addition and removal of the modification are generally termed histone acetyltransferases (HATs) and histone deacetylases (HDACs). However, in recent years, there has been a growing appreciation of the presence of lysine acetylation on other proteins, both nuclear and nonnuclear, suggesting a broader role of this PTM in vivo (Kim *et al.*, 2006; Choudhary *et al.*, 2009; Zhao *et al.*, 2010). One prominent example is the acetylation of the tumor suppressor p53 by coactivator CBP/p300, which markedly stimulates its DNA-binding activity, whereas its deacetylation by an HDAC1-containing complex represses p53-mediated transcriptional activation (Gu and Roeder, 1997; Luo *et al.*, 2000). Another example is tubulin acetylation via GCN5-related acetyltransferases (Akella *et al.*, 2010; Conacci-Sorrell *et al.*, 2010; Shida *et al.*, 2010), which is believed to play a role in microtubule dynamics and stability (reviewed in Janke and Bulinski, 2011). Such studies have broadened our view of lysine acetylation, suggesting that the assumption that an individual HAT or HDAC has an in vivo substrate range exclusive to histones may no longer hold validity. This has led to the use of the terms lysine acetyltransferases (KATs) and lysine deacetylases (KDACs), which are often used interchangeably with HATs and HDACs.

In comparison to the numerous acetyl-lysine sites that have been identified on diverse proteins (Kim *et al.*, 2006; Choudhary *et al.*, 2009; Weinert *et al.*, 2011), there are only a few HDAC-encoding genes (10 in *Saccharomyces cerevisiae* and 18 in *Homo sapiens*). This implies that each HDAC may have a significant number of physiological substrates. However, for the majority of the acetylated proteins, the biologically relevant HDACs remain largely unknown.

Partitioning of HDACs to different cellular compartments could be one important mechanism in defining their physiological function(s) and substrate range. In humans, HDAC6 is exclusively

This article was published online ahead of print in MBoC in Press (http://www.molbiolcell.org/cgi/doi/10.1091/mbc.E13-10-0619) on July 23, 2014.

Address correspondence to: Ruth N. Collins (ruth.collins@cornell.edu).

Abbreviations used: HAT, histone acetyltransferase; HDAC, histone deacetylase; SPB, spindle pole body; SPOC, spindle position checkpoint.

cytoplasmic, and it deacetylates both α-tubulin and cortactin to respectively regulate microtubule stability and actin-dependent cell motility (Hubbert *et al.*, 2002; Zhang *et al.*, 2007). HDAC6 also functions as an adaptor to target misfolded protein aggregates to the microtubule motor dynein, and the HDAC6 deacetylase activity is required for the aggresome formation (Kawaguchi *et al.*, 2003). In *Schizosaccharomyces pombe*, three HDACs (Clr3, Clr6, and Hda1) have distinct subcellular localization and in vivo specificity (Bjerling *et al.*, 2002). For the model organism of *S. cerevisiae*, the 10 HDAC genes are categorized into three classes: I (*RPD3*, *HOS1*, and *HOS2*), II (*HDA1* and *HOS3*), and III (*SIR2*, *HST1*, *HST2*, *HST3*, and *HST4*; Ekwall, 2005). The founding members of each class (*RPD3*, *HDA1*, and *SIR2*) have been extensively studied for their functions in processes such as gene expression, DNA damage response, and aging (Lin *et al.*, 2000; Keogh *et al.*, 2005; Robert *et al.*, 2011).

During our initial efforts to characterize the distribution of *S. cerevisiae* HDACs, we surprisingly discovered that a class II HDAC, Hos3, is specifically targeted to the mother-bud neck and to a single focus in the daughter cell. In addition to its localization, Hos3 appears unique in several aspects. Unlike other HDACs, which are functional only in the context of large complexes, Hos3 displays intrinsic deacetylase activity (Carmen *et al.*, 1999). Deletion of HOS3 results in little change in the global histone acetylation profile and causes no apparent phenotype (Carmen *et al.*, 1999; Robyr *et al.*, 2002). Unlike Rpd3 and Hda1, Hos3 is relatively insensitive to a classic HDAC inhibitor, trichostatin A (Carmen *et al.*, 1999). On oxidative stress, Hos3 is involved in mediating the induction of yeast apoptosis (Ahn *et al.*, 2006), although the normal physiological functions and substrates of Hos3 remain undiscovered. It is clear that Hos3 can function as a deacetylase capable of acting on histone tails when expressed in vitro (Carmen *et al.*, 1999). Moreover, the catalytic domain of Hos3 can replace Sir2 as an HDAC in heterochromatin establishment when targeted to the nucleus, indicating that Hos3 maintains deacetylase activity in vivo (Chou *et al.*, 2008).

In this study, we report that Hos3 displays asymmetric localization to the mother-bud neck and the daughter spindle pole body (SPB). Screening for mutants defective in targeting Hos3 to the neck identified septins and members of the morphogenesis checkpoint, pinpointing Hsl7 as the protein that recruits Hos3 to the bud neck. When a spindle orientation defect is present, Hos3 is loaded onto both SPBs, and its neck localization is important for this response. When associated with both SPBs, Hos3 may function as a spindle position checkpoint (SPOC) component to inhibit mitotic exit. We also uncover the mechanism behind the cell cycle–dependent asymmetric targeting of Hos3. The results together reveal how a uniquely localized lysine deacetylase, Hos3, functions as a link between the morphogenesis checkpoint and the SPOC and more generally substantiate roles for lysine acetylation and deacetylation in the regulation of mitotic exit.

RESULTS

Hos3 localizes asymmetrically to the bud neck and the daughter SPB

Ten HDAC genes can be recognized in the yeast genome. Two of the proteins encoded by these lysine deacetylase open reading frames, Hst2 and Hos3, are exclusively localized in the cytoplasm (Figure 1A). Hos3 displays a particularly striking and selective cytoplasmic localization pattern in vivo, being localized to a ring at the mother-bud neck and as a single focus in the daughter cell. The Hos3 localization pattern is identical for both NH_2- and COOH-terminally tagged Hos3 (Figure 1B, (i) and (ii)) and is unchanged whether Hos3 is integrated into the genomic locus or expressed ectopically from a plasmid (Figure 1B, (iii)). The Hos3 ring at the mother-bud neck has two distinctive features. First, Hos3 localizes selectively to the daughter side of the neck (Figure 1B). A number of proteins have been observed to adopt asymmetric localization at the bud neck (Cid *et al.*, 2002). For example, Bni4 is a mother-side-resident protein, whereas Kcc4 is anchored to the daughter side (Kozubowski *et al.*, 2005). Hos3 colocalizes with Kcc4 but not with Bni4, substantiating its asymmetric pattern of association (Figure 1C). A second feature of Hos3 neck localization is that the association appears stable in actively growing cells. We examined Hos3 neck localization with cells at different cell cycle stages (Figure 1D). On the onset of budding, Hos3 is immediately targeted to the neck and then remains associated throughout the remaining cell cycle (Figure 1D). These results show that the asymmetric pattern of bud-neck localization persists until cytokinesis. During cytokinesis, the daughter-side Hos3 ring splits into two separate rings (Figure 1D). By the completion of mitosis, Hos3 dissociates from previous bud sites and is not maintained on the bud scars (unpublished data). Hos3 does not associate with the mother side of the bud-neck ring even when overexpressed, suggesting the asymmetry is not due to a lack of intrinsic affinity to the mother side but that the machinery that directs Hos3 to the neck is itself asymmetric (Figure 1E).

The observed Hos3 focus in the daughter cell colocalizes with the daughter SPB, and Hos3 is not targeted to the mother SPB, revealing another pattern of asymmetry (Figure 1F). Of interest, asymmetric targeting of Hos3 onto the daughter SPB is cell cycle dependent (Figure 1F and Supplemental Movie S1). At early cell cycle stages, the sole SPB in the cell does not recruit Hos3 (Figure 1F, (i) and (ii)). After SPB duplication, both SPBs positioned within the mother cell are still devoid of Hos3 (Figure 1F, (iii)). Hos3 is loaded onto the daughter SPB only after the designated daughter SPB partitions into the cytoplasmic space of the growing daughter cell (Figure 1F, (iv) and (v)). Immediately after cytokinesis, Hos3 dissociates from the previous daughter SPB, and both cells again appear Hos3 free for their sole SPB.

Regions required for the specific targeting of Hos3

We performed serial truncations to map the regions essential for Hos3 localization at the bud neck and the daughter SPB (Figure 2). The single lysine deacetylase domain of Hos3 shares no homology to other class I and II HDACs outside the catalytic core (Supplemental Figure S1). The core deacetylase domain of Hos3 is located between residues 40 and 440 (Figure 2A). Outside the core deacetylase domain there is an NH_2-terminal 39–amino acid region and a COOH-terminal region of 257 amino acids. Neither the NH_2- nor the COOH-terminal region contains any distinguishing features that can be recognized from the primary amino acid sequence. Because of the absence of any identifiable features, we made truncation alleles of the COOH-terminal region, to create constructs that evenly truncated the protein approximately every 60 residues (Figure 2B). Truncation of the very COOH-terminal residues of 488–697 are dispensable for localization (Supplemental Figure S2, (i)–(iii)). However, deletions of the full COOH-terminus *CΔ* abolish localization, whereas *NΔ* still maintains Hos3 at the neck and daughter SPB (Supplemental Figure S2, (iv) and (v)). A combination deletion of *NΔ*+*CΔ*, which removes both the NH2- and COOH-termini, also is mislocalized (Supplemental Figure S2, (vi)). These data demonstrate that residues of 444–487 within the COOH terminus are necessary for Hos3 targeting.

The deacetylase domain also plays a role in Hos3 localization, since Hos3 lacking residues 40–443 (*HDACΔ*) is absent from the neck and daughter SPB (Supplemental Figure S2, (vii)). Almost all

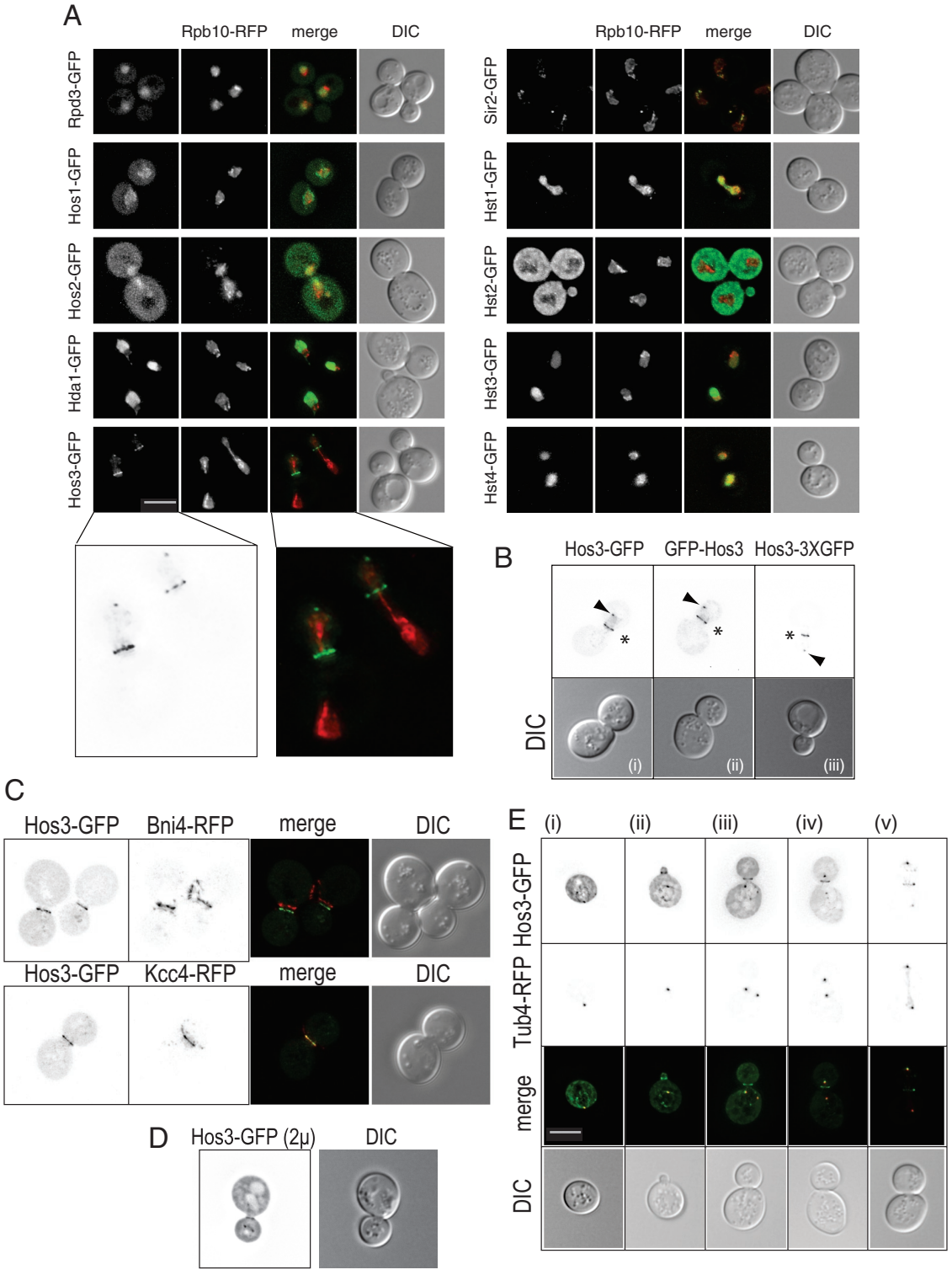

FIGURE 1: Unique targeting of Hos3. (A) Hos3 displays a unique localization pattern compared with other HDACs. All 10 HDACs of *S. cerevisiae*, fused with GFP and expressed from a single-copy *CEN* vector, were imaged in wild-type cells coexpressing the nucleus reporter Rpb10-RFP (*CEN*). An enlarged merged image of Hos3-GFP and Rpb10-RFP is also shown. Scale bar, 5 μm. (B) Cellular distribution of Hos3. Wild-type cells transformed with a single-copy *CEN* vector bearing Hos3-GFP (i), GFP-Hos3 (ii), or wild-type cells containing the endogenous copy of *HOS3* fused to three tandem copies of GFP (Hos3::3XGFP; iii) were analyzed by fluorescence microcopy. Asterisks denote Hos3 at the mother-bud neck. Arrowheads point to the Hos3 focus in the daughter cell. (C) Hos3 localizes to the daughter side of the bud neck. Wild-type cells transformed with Hos3-GFP (*CEN*) and the mother-side neck reporter Bni4-RFP (*CEN*) or the daughter-side neck reporter Kcc4-RFP (*CEN*) were analyzed by fluorescence microscopy. Images are represented as black on white to reveal the fine ultrastructure of Hos3 labeling with more clarity. (C) Hos3 associates with the bud neck throughout the cell cycle. Hos3-GFP (*CEN*) was imaged in wild-type cells at various cell cycle stages as revealed by a

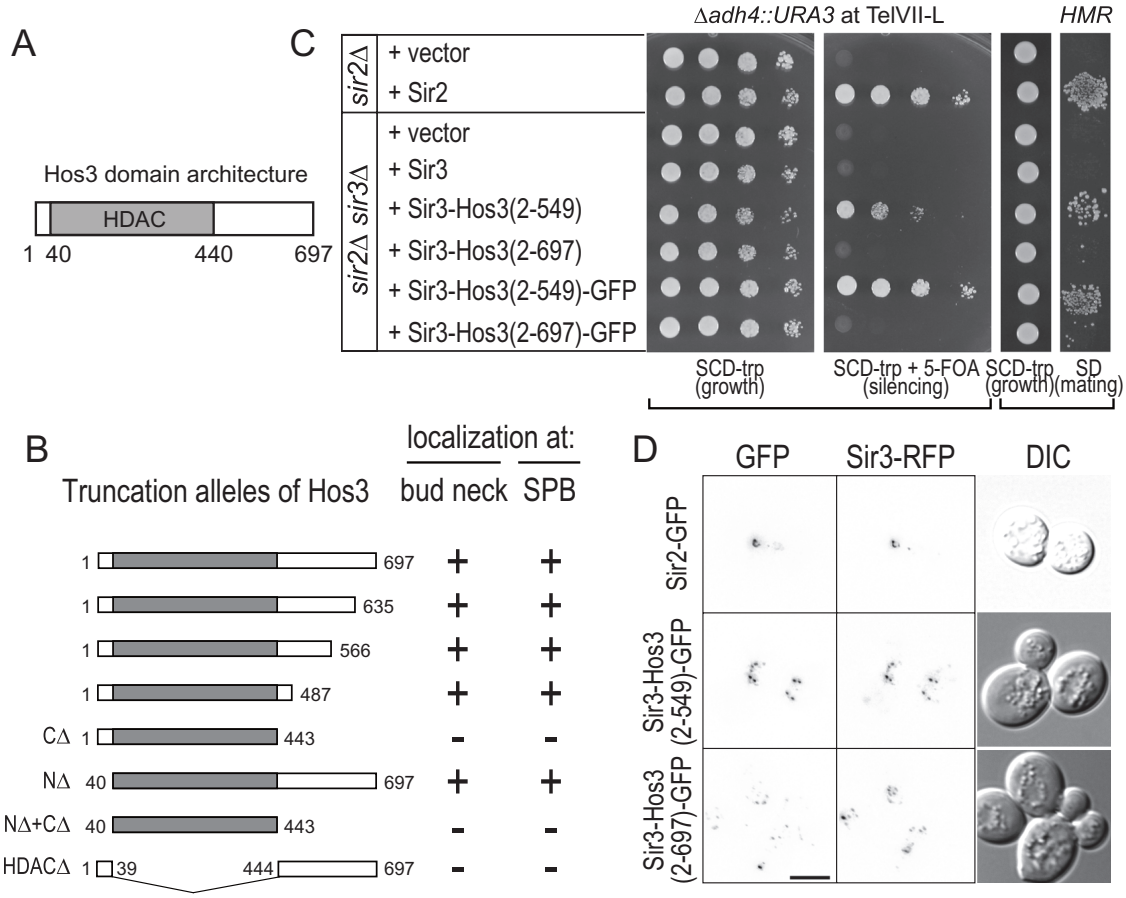

FIGURE 2: Domain and functional targeting of Hos3. (A) Domain analysis of Hos3. The HDAC domain comprises residues 40–440. (B) Mapping the region essential for Hos3 bud neck and daughter SPB localization. Full-length and systematically truncated versions of Hos3-GFP (*CEN*) were summarized for their capability of bud neck and daughter SPB targeting in wild-type cells. (C) Two Sir3-Hos3 chimeras differ in their ability to replace Sir2 as an HDAC. A copy of *URA3* was cloned into the subtelomeric region of chromosome VII in *sir2Δ* and *sir2Δ sir3Δ* cells. Cells transformed with an empty vector or *CEN* vectors bearing the corresponding genes were assayed by 10-serial dilution onto SCD-Trp and SCD-Trp + 0.1% 5-fluoroorotic acid (5-FOA) plates for incubation at 30°C or by mating with a MATa tester strain. Resistance to chemical 5-FOA indicates silencing of the *URA3* reporter; growth after replica onto the selective SCD plate reveals mating. (D) Targeting Sir3-Hos3 chimera to the Sir complex site correlates with its ability to catalyze deacetylation. Sir2-GFP (*CEN*), Sir3-Hos3(2-549)-GFP (*CEN*), and Sir3-Hos3(2-697)-GFP (*CEN*) were respectively imaged in wild-type cells coexpressing the Sir complex marker Sir3-RFP (*CEN*).

residues required for the proposed deacetylase catalytic mechanism are conserved between Hos3 and other lysine deacetylases (Supplemental Figure S3A; Finnin *et al.*, 1999). The in vivo ability of Hos3 to function as a lysine deacetylase has been elegantly demonstrated by its ability to substitute for Sir2 (Chou *et al.*, 2008). Maintenance of the heterochromatin requires the Sir complex (Sir2/3/4; Rusche *et al.*, 2003). In the absence of the HDAC Sir2, cells fail to silence a *URA3* reporter cloned into the subtelomeric region or to mate properly (Chou *et al.*, 2008). Fusion of the heterologous Hos3 with the adaptor protein Sir3 was shown to bypass endogenous Sir2 and reverse the defect in silencing and mating in *sir2Δ* mutants (Chou *et al.*, 2008). In this situation the Sir3-Hos3 fusion targets the catalytic domain of Hos3 to the Sir complex sites and can reverse the silencing or mating defects. Mutation of conserved catalytic residues renders the Sir3-Hos3 chimera unable to replace Sir2 (Supplemental Figure S3, B and C). Loss of deacetylase activity does not perturb either the Hos3 protein level or its localization pattern (Supplemental Figure S3, D and E).

In the case of the two chimeras, Sir3-Hos3(2-549) but not Sir3-Hos3(2-697) can replace Sir2 as a functional HDAC (Figure 2C; Chou *et al.*, 2008). Because the normal endogenous Hos3 is localized to the bud neck and SPB, we investigated the localization of these two

growing size of the bud. The images are rotated with the bud neck parallel to the horizontal axis. (D) Hos3-GFP expressed from a high-copy 2μ vector was imaged in wild-type cells. (E) Localization pattern of Hos3 throughout the cell cycle. Wild-type cells transformed with Hos3-GFP (*CEN*) and the SPB marker Tub4-RFP (*CEN*) were analyzed by fluorescence microcopy. Cells are shown at various cell cycle stages: i) unbudded, ii) budding, iii) post SPB duplication, iv) spindle elongation, and v) nuclear segregation. The images are rotated with the bud neck parallel to the horizontal axis. Tub4-RFP appropriately labels the SPBs but not the kinetochores.

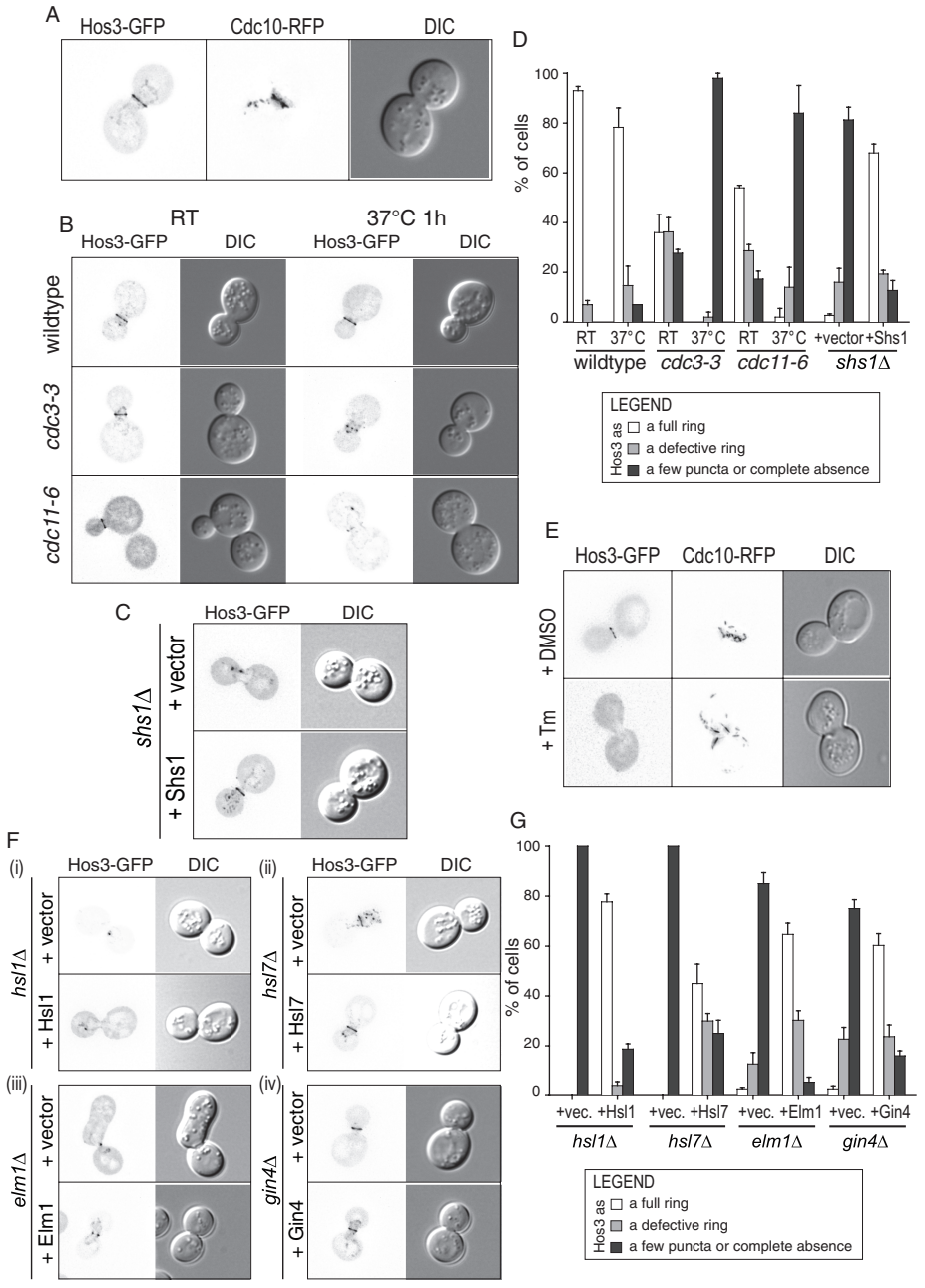

FIGURE 3: Septins and four proteins identified via mutant screening are required to target Hos3 to the bud neck. (A) Wild-type cells transformed with Hos3-GFP (*CEN*) and the septin reporter Cdc10-RFP (*CEN*) were analyzed by fluorescence microcopy. (B, C) Septins are required to target Hos3 to the bud neck. (B) Hos3-GFP (*CEN*) was imaged in wild-type cells or heat-sensitive *cdc3-3* and *cdc11-6* septin mutants at room temperature (RT) and after 1-h shift to restrictive temperature (37°C). (C) Hos3-GFP (*CEN*) was imaged in *shs1Δ* cells transformed with an empty vector or a *CEN* vector bearing Shs1. (D) Quantification of data from B and C. Cells were categorized into three groups based on the pattern of Hos3 at the neck. $N = 300$ cells. The error bar represents SEM. (E) Wild-type cells transformed with Hos3-GFP (*CEN*) and Cdc10-RFP (*CEN*) were analyzed by fluorescence microcopy after 2 h of treatment with dimethyl sulfoxide (DMSO) or 2 μg/ml tunicamycin (Tm) at 30°C. (F) Screening identified four mutants deficient in Hos3 neck association. Hos3-GFP (*CEN*) was imaged in i) *hsl1Δ*, ii) *hsl7Δ*, iii) *elm1Δ*, and iv) *gin4Δ* cells transformed with an empty vector or a single-copy vector bearing a copy of the wild-type gene as control. (G) Quantification of cells in F was performed as in D.

Sir3-Hos3 fusion proteins. The functional Sir3-Hos3(2-549)–green fluorescent protein (GFP) chimera is correctly targeted to the Sir complex sites, but the nonfunctional Sir3-Hos3(2-697)-GFP chimera is not (Figure 2, C and D). Therefore the reason Sir3-Hos3(2-697) appears nonfunctional in this assay is most likely due to a targeting rather than an enzymatic defect. The Sir3-Hos3 chimera data demonstrate that the core domain of Hos3 can act as a lysine deacetylase when forced to the sites of Sir2 function. Together these results suggest that Hos3, which normally localizes to the bud neck and the daughter SPB, is likely to function as a lysine deacetylase at these specific sites. The regions that enable Hos3 to reside at the mother-bud neck and SPB are located outside the core catalytic domain. The unique localization pattern of endogenous Hos3 therefore likely reflects its action on nonnuclear targets.

Septins and four regulators are required for Hos3 localization at the bud neck

We next examined the mechanism by which Hos3 is recruited to the bud neck. Hos3 is a soluble protein, and sequence analysis reveals no potential transmembrane or lipid-binding domain. Neither microtubule depolymerization by nocodazole nor inhibition of actin filament assembly by latrunculin B caused any change of Hos3 neck localization (unpublished data). However, we found that septins are necessary for the bud neck localization of Hos3. Septin subunits assemble into high-order filaments and form an hourglass structure at the bud neck, serving as a scaffold to recruit other proteins and as a diffusion barrier between the mother and daughter cells (reviewed in Oh and Bi, 2011). Hos3 colocalizes with septins (Figure 3A). Inactivation of two essential septin subunits (Cdc3 and Cdc11) or deletion of the nonessential subunit (Shs1) results in the loss of Hos3 full-ring pattern at the neck (Figure 3, B–D). Septin morphology can also be perturbed by tunicamycin (Tm) treatment (Babour *et al.*, 2010). Accordingly, Hos3 dissociates from the neck upon addition of Tm (Figure 3E). These results demonstrate that the localization of Hos3 at the mother-bud neck is septin dependent.

Although septins are necessary for Hos3 neck localization, we wanted to know whether septins act directly or indirectly in Hos3 neck recruitment, as septin neck association is an established requirement for other proteins known to associate in this region. To uncover how Hos3 is localized to the neck, we took a targeted approach and screened a pool of ~120 mutants covering genes important for bud-neck assembly, cell-cycle regulation, and polarity establishment (Drees *et al.*, 2001; Markus and Lee, 2011; Howell and Lew, 2012; Supplemental Table S1). Four mutants were identified as hits from our screen: *hsl1Δ*,

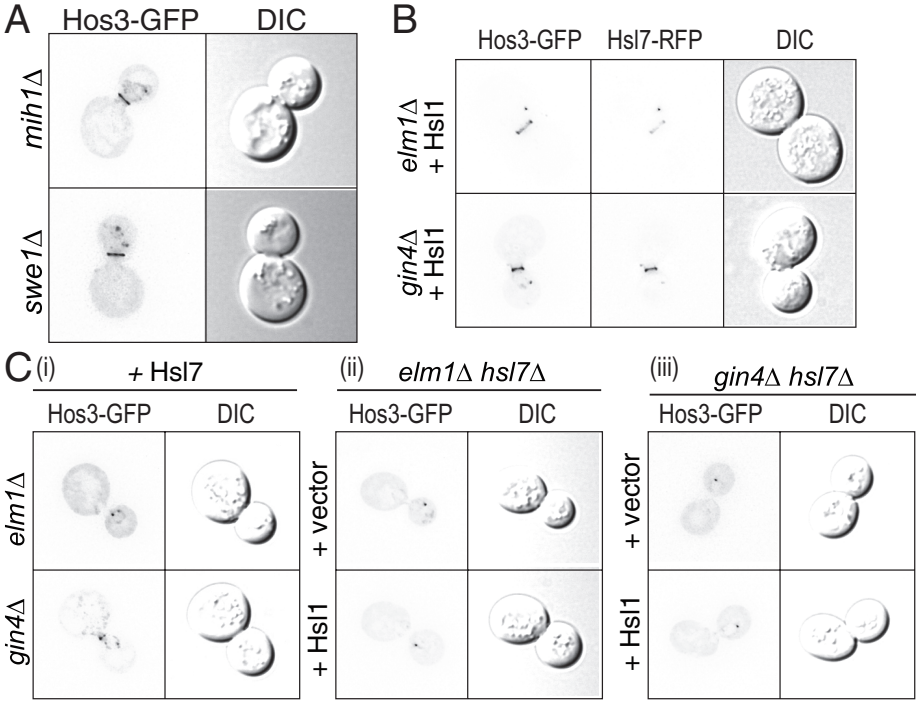

D

RFP-tagged protein localization

strain \ RFP	Cdc10	Hsl1	Hsl7	Elm1	Gin4
wildtype	+++	+++	+++	+++	+++
shs1Δ	+	-/+	-/+	-/+	++
hsl1Δ	++	+++	-	+++	+++
hsl7Δ	++	+++	+++	+++	+++
elm1Δ	-/+	+++	-/+	+++	++
gin4Δ	+	+++	-/+	+	+++

pattern

vs.

Localization pattern at the bud neck

strain	Hos3-GFP localization				
wildtype	+++	+++	+++	+++	+++
shs1Δ	-/+	-/+	-/+	-/+	-/+
hsl1Δ	-	+++	-	-	-
hsl7Δ	-	-	+++	-	-
elm1Δ	-/+	+++	-/+	+++	-/+
gin4Δ	-/+	+++	-/+	-/+	+++

pattern

FIGURE 4: The Hsl1-Hsl7 module of the morphogenesis checkpoint regulates Hos3 neck localization. (A) Localization of Hos3-GFP (*CEN*) in *mih1Δ* and *swe1Δ* cells. (B) Increasing the level of active Hsl1 rescues Hos3 to the neck. Hos3-GFP (*CEN*) was imaged in *elm1Δ* and *gin4Δ* cells transformed with a *CEN* vector bearing Hsl1. Hsl7-RFP localization is shown for comparison, as the increased level of Hsl1 also restores Hsl7 bud-neck association. (C) Rescue of Hos3 neck localization with active Hsl1 requires both the presence and neck association of Hsl7. (i) Increasing Hsl7 levels by providing an extra copy of Hsl7 in *elm1Δ* and *gin4Δ* cells does not restore Hos3-GFP (*CEN*) neck localization. (ii) Hos3-GFP (CEN) was imaged in double-mutant *elm1Δ hsl7Δ* and *gin4Δ hsl7Δ* cells transformed with an empty vector or a *CEN* vector bearing Hsl1. (D) Summary of the reciprocal localization profile. Cells (Supplemental Figure S6, A–F) were recorded for the neck patterns of Hos3 and its regulators. The first group examined the neck localization of the RFP marker in cells with the genotype indicated on the left, transformed with the different marker plasmids indicated in the header. The second group displays the pattern of Hos3 localization assayed simultaneously in the same cells. The localization pattern was assigned into one of four categories as indicated: –, absence from the neck; +, as a defective ring; ++, as an incomplete ring; +++, as a full ring at the neck.

hsl7Δ, *elm1Δ*, and *gin4Δ*. Hos3 is completely absent from the neck in *hsl1Δ* and *hsl7Δ* cells (Figure 3, F, (i) and (ii), and G). The localization defect is less severe in *elm1Δ* and *gin4Δ* cells, where Hos3 fails to form a full ring (Figure 3, F, (iii) and (iv), and G). Reintroduction of each deleted gene from a plasmid rescues Hos3 localization to the neck as a full ring (Figure 3, F and G). The level of Hos3 is comparable between wild-type cells and the four hit mutants, arguing that the observed localization defect is not due to Hos3 down-regulation (Supplemental Figure S4A). Hsl1, Hsl7, Elm1, and Gin4 are all neck-localized proteins and thus could play a structural role in targeting Hos3.

In addition to Hsl1 and Gin4, Kcc4 is a third member of the partially redundant Nim1-related kinases (Longtine *et al.*, 1998; Barral *et al.*, 1999). However, Hos3 showed no localization defect in *kcc4Δ* mutant cells (Supplemental Figure S4B). Similarly, Hos3 localization was unperturbed in a mutant of another kinase, Cla4, that localizes to the neck and is involved in septin filament assembly and localization (Weiss *et al.*, 2000; Versele and Thorner, 2004; Supplemental Figure S4B). These data suggest that the four hits from the screening are specific regulators of Hos3 neck localization.

The Hsl1-Hsl7 module of the morphogenesis checkpoint targets Hos3 to the neck

All four of the identified genes responsible for Hos3 neck localization are involved in the regulation of morphogenesis (Blacketer *et al.*, 1993; Longtine *et al.*, 1998; Lew and Burke, 2003). Together with septins, these proteins are part of an integrated morphogenesis checkpoint that monitors the coordination between bud growth and mitotic entry (Lew, 2000; Lew and Burke, 2003; Keaton and Lew, 2006; Howell and Lew, 2012).

To delineate how Hos3 responds to the action of Elm1, Gin4, Hsl1, and Hsl7, we wanted to understand how Hos3 neck recruitment responds to the established signal transduction framework of the morphogenesis checkpoint. Deletion of either *MIH1* or *SWE1* had no effect on Hos3 neck localization (Figure 4A). Furthermore, inactivation of the morphogenesis checkpoint causes a Swe1-dependent G2 delay, but release of this cell cycle delay in the septin or hit mutants does not restore Hos3 full-ring localization (Supplemental Figure S5A). Hos3 is a potential Cdc28 substrate, so it is possible that phosphorylation by Cdc28 is required for Hos3 neck localization (Holt *et al.*, 2009). However, Hos3 with all four Cdc28 consensus sites mutated to alanine displays a wild type-like pattern of localization (Supplemental Figure S5B). These data suggest that the recruitment of Hos3 to the neck is upstream of cyclin-dependent kinase (CDK) regulation.

Remarkably, an extra copy of plasmid-borne Hsl1 rescues Hos3 to the neck as a full ring in *elm1Δ*, *gin4Δ* (Figure 4B), and even *elm1Δ gin4Δ* double-mutant cells (Supplemental Figure S5C). The rescue

effect is dependent on Hsl1 kinase activity (Supplemental Figure S5D; Theesfeld *et al.*, 2003). These results indicate that for Hos3 assembly at the neck, the loss of Hsl1 activation by upstream Elm1 and Gin4 could be compensated by increasing the level of Hsl1 to bring Hsl1 activity over a threshold sufficient to enable neck recruitment. Hsl1 restored to the neck further recruits both Hsl7 and Hos3 (Figure 4B). These data indicated that the recruitment of Hos3 to the neck is downstream of Elm1 and Gin4 action.

The Hsl1 overexpression rescue phenotype appeared dependent on the ability of Hsl1 to restore Hsl7 to the neck because the same rescue effect could not be obtained by simply increasing the levels of Hsl7 in *elm1Δ* or *gin4Δ* mutant cells, a situation in which Hsl7 is unable to be recruited to the bud neck (Figure 4C, (i)). Neither could rescue be achieved by expressing an extra copy of Hsl1 in *elm1Δ hsl7Δ* or *gin4Δ hsl7Δ* double-mutant cells (Figure 4C, (ii)). All of the foregoing data suggest that the recruitment of Hos3 to the neck is downstream of Elm1 and Gin4 action and directly dependent on the Hsl1-Hsl7 module.

To further dissect the genetic network responsible for Hos3 neck localization (septins and genes identified by screening), we performed a reciprocal localization study (Figure 4D and Supplemental Figure S6, A–F). We recorded the neck localization patterns for both Hos3 and a member of the genetic network for each mutant strain indicated. A summary of these pairwise observations is shown in Figure 4D. The 30 pairs of observations were divided into two groups. The first group examined the neck localization of a red fluorescent protein (RFP)–tagged copy of each individual member of the network responsible for Hos3 localization. The second group simultaneously assayed the pattern of neck Hos3 localization. Each RFP marker and Hos3-GFP pair was recorded for mutants of all genes in the network (*shs1Δ* cells were used as a representative of septin mutants). As expected, a marker plasmid expressed in a mutant cell line of that particular gene has normal localization of both itself and Hos3. As described in the preceding sections, pairwise observations indicated the dependence of Hos3 neck localization on the septins and *HSL1*, *HSL7*, *ELM1*, and *GIN4* genes. Of this set of genes, the marker whose localization profile most closely resembles the patterns of Hos3 localization was Hsl7. Not only does Hsl7 display the best pattern match, we found that whenever Hsl7 and Hos3 markers were examined simultaneously, Hos3 was always observed with Hsl7 at the bud neck (Supplemental Figure S6, A–F, row 3). The Hsl1 localization pattern partially matches that of Hos3, with the exception of *hsl7Δ* cells (Supplemental Figure S6D, row 2). Moreover, Hsl1 and Hsl7, similarly to Hos3, localize only to the daughter side of the neck (septins localize to both sides; Elm1 and Gin4 are situated in the middle of the bud neck; Supplemental Figure S6A). Of even more interest, targeting of both Hsl1 and Hsl7 to the neck is largely abolished in *shs1Δ*, *elm1Δ*, and *gin4Δ* mutants, suggesting that septins, Elm1, and Gin4 are required for Hos3 neck localization only because they function upstream of Hsl1 and Hsl7 to recruit this module to the bud neck.

Neck-localized Hsl7 binds and recruits Hos3

Our experimental data suggested three mutually exclusive scenarios for the involvement of the Hsl1-Hsl7 module in Hos3 neck recruitment: 1) Hsl1 alone, 2) Hsl1 and Hsl7 together, or 3) Hsl7 alone is responsible for the recruitment of Hos3 to the neck. In the absence of *HSL7*, Hsl1 localizes as a full ring at the neck but is insufficient to target Hos3, arguing against the first scenario (Supplemental Figure S6D, row 2). Consistent with the other two scenarios in which Hsl7 is required, deletion of *HSL7* completely abolishes the ability of overexpressed Hsl1 to rescue Hos3 neck localization (Figure 4, C, (ii), compared with B).

We next determined whether the involvement of Hsl1 was a result of its ability to target Hsl7 to the bud neck (McMillan *et al.*, 1999; Shulewitz *et al.*, 1999). Hsl1 physically associates with Hsl7, suggesting that Hos3 recruitment could be directly or indirectly dependent on Hsl1. We tested this by using an Hsl7K254E mutant that fails to bind Hsl1 (Cid *et al.*, 2001). The inability of Hsl1 to associate with Hsl7K254E results in the failure to target Hos3 to the bud neck (Figure 5A). This suggests that Hsl1 functions in Hos3 bud-neck recruitment via its ability to recruit Hsl7. To examine this question, we created a cell line in which Hsl7 was targeted to the bud neck in an Hsl1-independent mechanism. Fusing Hsl7 to the bud neck kinase Gin4 creates a chimera that localizes to the neck independent of endogenous Hsl7 or Hsl1 (Figure 5B). The Hsl7 portion of the chimera is able to rescue Hos3 to the neck in *hsl7Δ* mutant cells (Figure 5B, top). The Gin4-Hsl7 chimera also targets Hos3 to the neck in the *hsl1Δ* mutant (Figure 5B, bottom). Therefore neck-localized Hsl7 alone is sufficient to recruit Hos3. Hsl1 is necessary for Hos3 neck recruitment due to its function in targeting and activating Hsl7 at the neck; recruitment of Hsl7 in a manner independent of Hsl1 is able to bypass this requirement.

These results strongly argue for a direct physical interaction between Hsl7 and Hos3 at the neck. We examined this possibility with two independent methods. First, we looked for physical association between the two proteins and were able to coimmunoprecipitate endogenous Hos3 with endogenous Hsl7 (Figure 5C). Second we tested whether the physical interaction between Hsl7 and Hos3 could be confirmed in vivo. Sec2, a guanine nucleotide exchange factor for Rab GTPase Sec4, is involved in post-Golgi exocytosis and is localized on polarized secretory vesicles (Figure 5D, top; Walch-Solimena *et al.*, 1997). In wild-type cells, endogenous Hsl7 recruits Hos3 to the neck, and an exogenous Sec2-Hsl7 chimera is sufficient to target Hos3 to the post-Golgi vesicles (Figure 5D, bottom). Deletion of *HSL7* or *HSL1* in cells expressing the Sec2-Hsl7 chimera results in Hos3 dissociation from the neck but not from the vesicles (Figure 5E). In conclusion, Hsl7 physically interacts with and recruits Hos3 to the bud neck.

Understanding the role of neck-localized Hos3

Having uncovered the mechanism that asymmetrically targets Hos3 to the bud neck, we sought to understand how this could affect the physiological functions of Hos3. Hos3 is not involved in assembling septins and is not required for Gin4, Elm1, Hsl1, or Hsl7 recruitment at the bud neck, suggesting it acts downstream of the septins and septin-associated morphogenesis network (Supplemental Figure S7A). We also observed no cytokinesis defect in *hos3Δ* cells (unpublished data). Therefore Hos3 does not appear to play an essential structural role at the bud neck. We next examined whether Hos3 could be a member of the morphogenesis checkpoint. Deletion of *HSL1* or *HSL7* inactivates the morphogenesis checkpoint and results in a G2 delay, but *hos3Δ* cells are not enriched for the G2/M subpopulation (Supplemental Figure S7B). In a different W303 strain background, the G2 delay of *hsl7Δ* cells is readily apparent from their elongated morphology and temperature sensitivity, whereas *hos3Δ* cells display neither of these defects (Supplemental Figure S7, C and D). Therefore, whereas the morphogenesis checkpoint is important in targeting Hos3 to the neck, Hos3 does not appear to be a member of this signaling pathway.

Another attractive hypothesis is that neck localization is required to load Hos3 asymmetrically onto the daughter SPB. However, Hos3

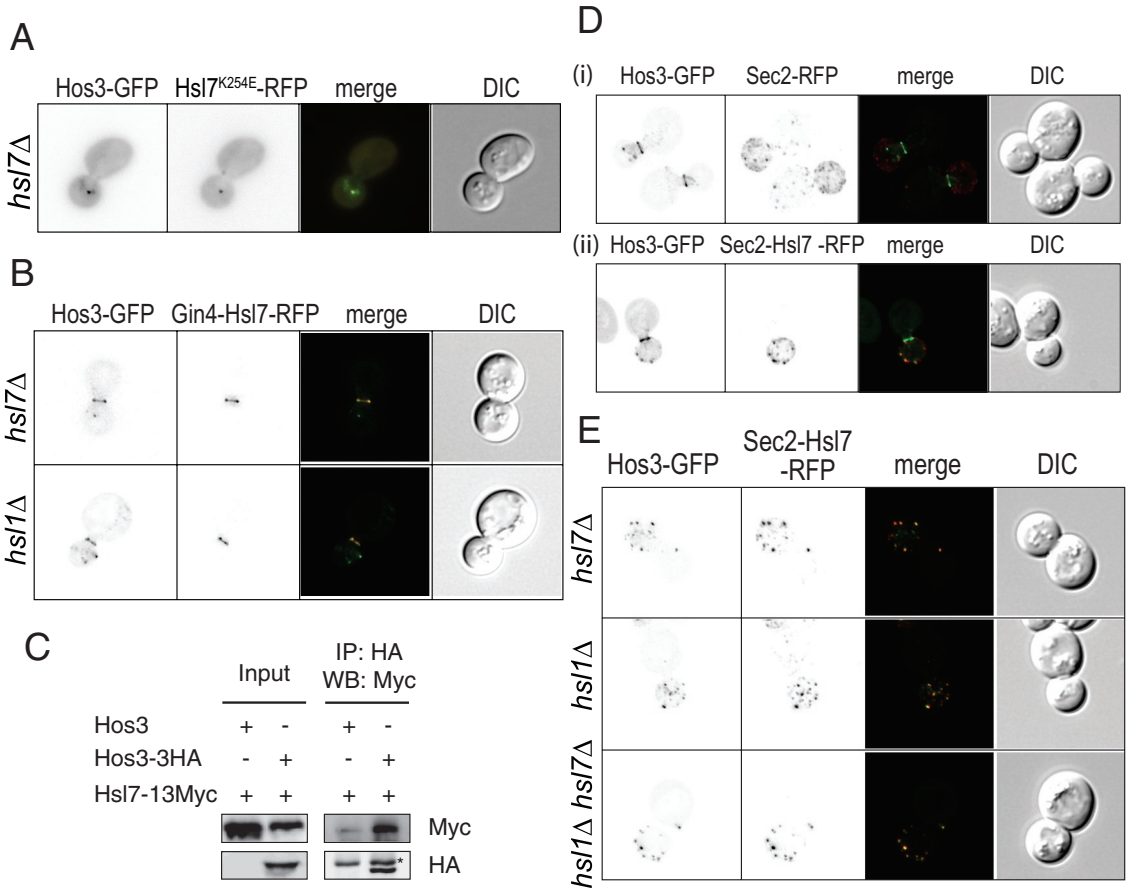

FIGURE 5: Hsl7 alone recruits Hos3 to the bud neck. (A) Failure to target Hsl7 to the neck abolishes Hos3 neck localization. Hos3-GFP (*CEN*) was imaged in *hsl7Δ* cells containing a *CEN* plasmid bearing Hsl7K254E. (B) Neck-localized Hsl7 bypasses Hsl1 for Hos3 neck targeting. *hsl7Δ* and *hsl1Δ* cells transformed with Hos3-GFP (*CEN*) and a chimera of Gin4-Hsl7-RFP (*CEN*) were analyzed by fluorescence microcopy. (C) Hos3 interacts with Hsl7. Cells of which endogenous Hsl7 is fused with 13 copies of Myc tag and endogenous Hos3 is either untagged or fused with three copies of HA tag were grown to mid–log phase in YPD medium and lysed for immunoprecipitation with anti-HA agarose resin. The resin was eluted with SDS–PAGE sample buffer and analyzed by immunoblotting against HA or Myc epitope tag. The star denotes a nonspecific band originating from resin-attached anti-HA antibodies. (D, E) Hsl7 is sufficient to direct Hos3 localization. Hos3-GFP (*CEN*) and Sec2-RFP (*CEN*) were coimaged in wild-type cells (D, (i)). Hos3-GFP (*CEN*) and a chimera of Sec2-Hsl7-RFP (*CEN*) were coimaged in wild type cells (D, (ii)) or *hsl7Δ*, *hsl1Δ*, and *hsl1Δ hsl7Δ* cells (E). Triangles indicate the sites of colocalization between Hos3-GFP and the exocytic vesicles marked with the Sec2-Hsl7-RFP chimera.

is correctly targeted onto the daughter SPB in *hsl7Δ* cells (Supplemental Figure S7E). Finally, deletion of several HDACs, including *HOS3*,suppresses the temperature sensitivity of a strain containing a mutation in the anaphase-promoting complex, *apc5CA* (Turner *et al.*, 2010). In contrast, deletion of *HSL7* fails to do so, indicating that neck localization is dispensable for this Hos3-associated genetic interaction (Supplemental Figure S7F).

To understand Hos3 function further, we decided to examine more closely a striking aspect of Hos3 asymmetric association with the daughter SPB (Figure 1F). The SPBs organize cytoplasmic microtubules, which, together with motor proteins, are instrumental for positioning and segregating the nucleus (Jaspersen and Winey, 2004). A selective association with the daughter SPB indicates that Hos3 has the ability to discriminate between the two SPBs. In yeast, these are asymmetrically positioned in the mother and daughter cells, with the mother cell retaining the newly duplicated SPB. Loss of the cytoplasmic dynein heavy chain Dyn1 results in a significant number of cells with misaligned spindles (Li *et al.*, 1993). In this situation the SPBs may not be partitioned between the mother and daughter cells. We asked what would happen to Hos3 SPB localization under these conditions. Of interest, we found that Hos3 is loaded onto both SPBs in *dyn1Δ* cells with misaligned spindles (Figure 6A, (i)). In comparison, for the fraction of dyn1*Δ* cells that possess well-aligned spindles, Hos3 is still observed to be asymmetrically targeted onto the daughter SPB as seen in wild-type cells (Figure 6A, (ii) and (iii)). Besides dynein, the dynactin complex and the cortical protein Num1 are also essential for positioning the nucleus (Heil-Chapdelaine *et al.*, 2000). Loss of dynactin components (Arp1, Jnm1, and Nip100) or Num1 also gives rise to cells with misaligned spindles. In these mutant cells, Hos3 was similarly targeted onto both SPBs (Figure 6B). Furthermore, pharmacological intervention with nocodazole inhibits microtubule polymerization and formation of the spindle, resulting in SPB coalescence, observable as a single focus that contains both SPBs. Similarly, in nocodazole-treated

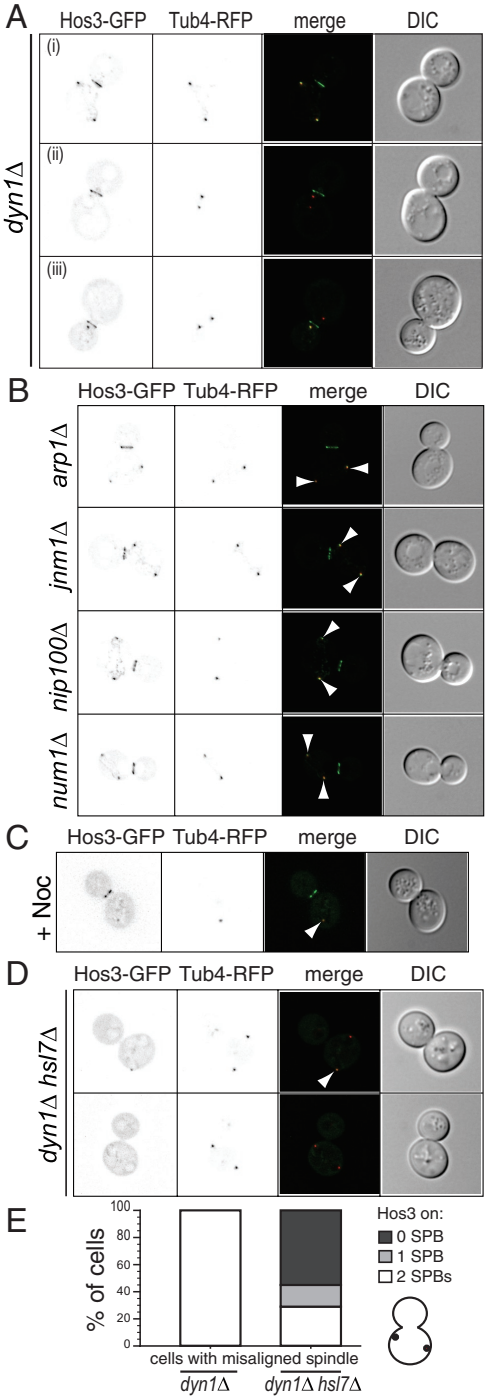

FIGURE 6: Loading of Hos3 onto both SPBs in response to spindle orientation defects. (A) Hos3-GFP (*CEN*) and Tub4-RFP (*CEN*) were coimaged in *dyn1Δ* cells. Shown are cells with misaligned spindle (i) or with spindles that are normally aligned (ii and iii). Arrowheads point to Hos3 on both SPBs (i) or on the daughter SPB (iii). (B) Hos3-GFP (*CEN*) and Tub4-RFP (*CEN*) were coimaged in *arp1Δ*, *jnm1Δ*, *nip100Δ*, and *num1Δ* cells. Shown are cells with misaligned spindle. Arrowheads point to Hos3 on both SPBs. (C) Wild-type cells transformed with Hos3-GFP (*CEN*) and Tub4-RFP (*CEN*) were treated with 40 µg/ml nocodazole (Noc) for 3 h at 30°C and then analyzed by fluorescence microscopy. Owing to microtubule depolymerization, the spindle collapsed and the two SPBs remained close, appearing as one focus. Hos3 on the SPBs is indicated with an arrowhead. (D) Neck targeting is required for the loading of Hos3 onto both SPBs in response to spindle misorientation. Hos3-GFP (*CEN*) and Tub4-RFP (*CEN*) were coimaged in *dyn1Δ hsl7Δ* cells. Shown are cells with misaligned spindle that load Hos3 onto only one or none of the two SPBs. Arrowhead points to Hos3 on one SPB. (E) Quantification of cells with misaligned spindle in A and D. Cells were categorized into three groups based on association of Hos3 with none, only one, or both of the two SPBs. *N* = 100 cells with misaligned spindle.

cells, Hos3 can be observed as a single focus (Figure 6C). These data indicate that Hos3 is normally asymmetrically localized but can be symmetrically loaded onto both SPBs in response to a spindle orientation defect.

We next asked whether Hos3 neck localization would be required for its response to spindle misorientation. Deletion of *HSL7* abolishes Hos3 association with the bud neck in *dyn1Δ* cells, and, of interest, *dyn1Δ hsl7Δ* cells with misaligned spindles become unable to efficiently load Hos3 onto both SPBs (Figure 6, D and E). These data suggest that Hsl7 is essential for the response, and neck-localized Hos3 may function as a "sensor" of the spindle orientation defect and facilitate a cellular response by loading Hos3 onto both SPBs.

Hos3 is a novel component of the spindle position checkpoint

At least three other proteins (Bub2, Bfa1, and Kin4) are known to bind both SPBs in cells with misaligned spindles (D'Aquino *et al.*, 2005; Pereira and Schiebel, 2005). Bub2 and Bfa1 together act as a two-component GTPase-activating protein (GAP) that negatively regulates Tem1 GTPase, a key regulator of the mitotic exit network (MEN; Bardin and Amon, 2001). Kin4 functions as another negative regulator of the MEN through phosphorylating Bfa1 and preventing its inactivation by Cdc5 polo-like kinase (D'Aquino *et al.*, 2005; Pereira and Schiebel, 2005; Maekawa *et al.*, 2007) These three proteins are all members of the SPOC, which monitors spindle orientation before committing the cell to mitotic exit (Caydasi *et al.*, 2010a). The SPOC inhibits the activation of the MEN until the mitotic spindle is aligned properly along the mother-bud axis; when the spindle is misaligned, the SPOC causes cells to arrest at anaphase (Caydasi *et al.*, 2010a).

In response to spindle misorientation, SPOC members are loaded onto both SPBs to act as a brake upon the MEN (D'Aquino *et al.*, 2005; Pereira and Schiebel, 2005). Given its similar SPB association feature, we asked whether Hos3 could function as a SPOC component. Inactivation of the SPOC by loss of Bub2, Bfa1, or Kin4 causes cells with misaligned spindles to nevertheless exit mitosis, so the cell population is reduced for "arrested" but increased for "bypassed" spindle morphology (D'Aquino *et al.*, 2005). Similarly, upon loss of Hos3, cells with misaligned spindles were defective in mitotic arrest and enriched for the "bypassed" subpopulation (Figure 7A). Of interest, *dyn1Δ hsl7Δ* cells are also compromised for the SPOC, consistent with the requirement of neck-localized Hos3 to respond to spindle misalignment (Figure 7A). The lysine deacetylase activity is required for Hos3 to function in the SPOC, as cells with a Hos3 allele containing point mutations in two key catalytic residues, Hos3$^{H196E,\ D231N}$, are unable to promote mitotic arrest (Figure 7B). These data suggest that upon spindle misorientation, Hos3 is loaded onto both SPBs to deacetylate potential substrate(s) and inhibit mitotic exit.

Spindle misorientation activates the SPOC by loading its components onto both SPBs. Consequently, for cells with well-aligned spindles, constitutive association of SPOC components with both SPBs would still inhibit mitotic exit. Indeed, when overexpressed, Bub2 mildly inhibits cellular growth, whereas Bfa1 or Kin4 causes

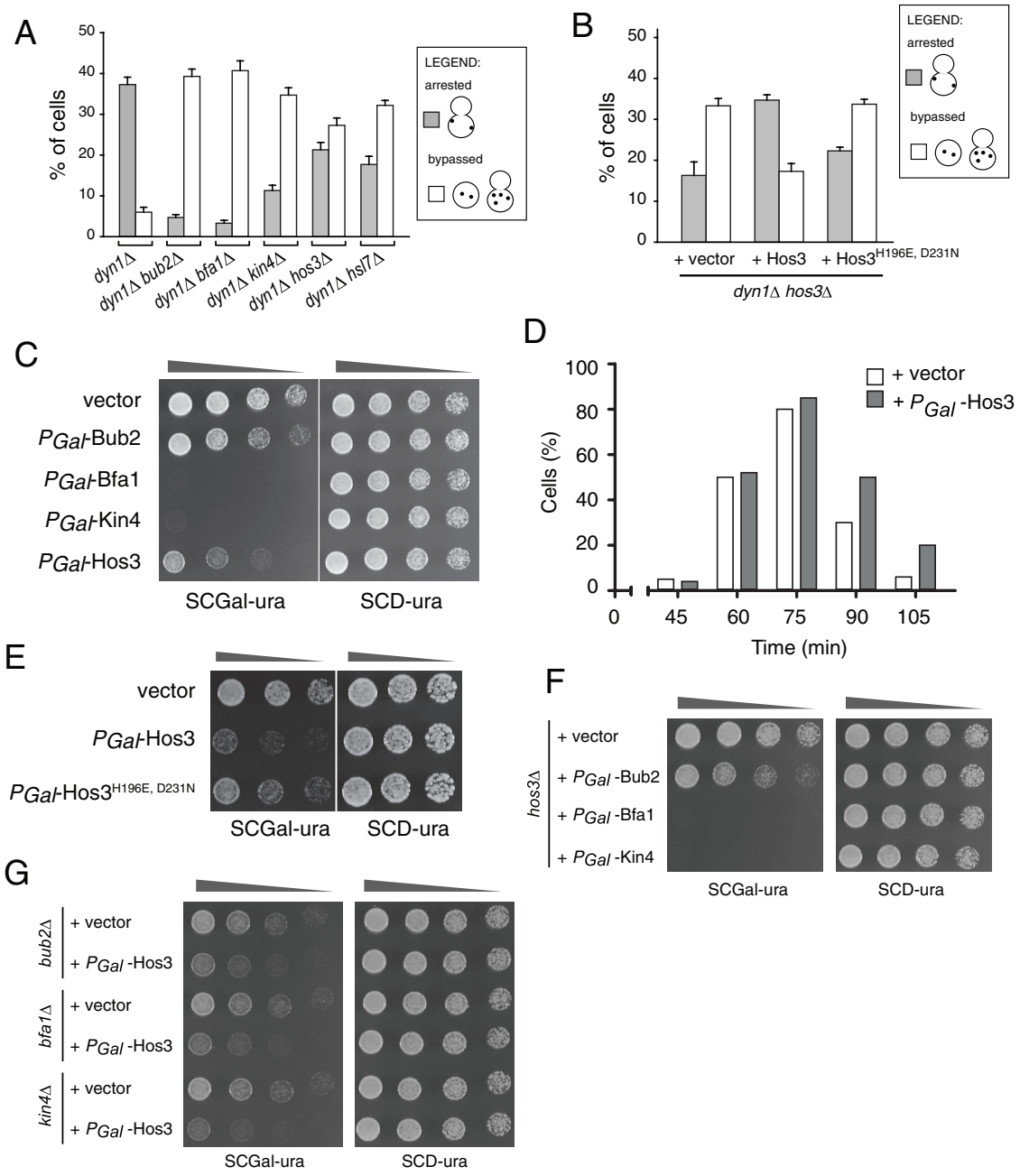

FIGURE 7: Hos3 inhibits mitotic exit when loaded onto both SPBs. (A) *dyn1Δ*, *dyn1Δ bub2Δ*, *dyn1Δ bfa1Δ*, *dyn1Δ kin4Δ*, *dyn1Δ hos3Δ*, and *dyn1Δ hsl7Δ* cells, transformed with the SPB reporter Tub4-RFP (*CEN*), were grown to early mid–log phase in synthetic minimal medium, switched to 14°C for 20 h, and analyzed by fluorescence microcopy for "arrested" or "bypassed" spindle morphology. One hundred cells were analyzed for each genotype. Cells containing aberrant spindle morphologies were categorized as either arrested (cells are arrested with misaligned spindle) or bypassed (cells containing a misaligned spindle nevertheless exit mitosis, thus giving rise to unbudded cells with two SPBs as well as cells with more than two SPBs when these unbudded cells start to grow). (B) *dyn1Δ hos3Δ* cells transformed with the SPB reporter Tub4-RFP (*CEN*) and cotransformed with an empty vector, Hos3 (*CEN*), or Hos3H196E,D231N (*CEN*) were analyzed as in A. (C) Wild-type cells, transformed with an empty vector or 2μ vectors bearing Bub2, Bfa1, Kin4, and Hos3 all driven under a galactose-inducible promoter, were grown to mid–log phase in synthetic raffinose medium (–Ura) and analyzed by three-serial dilution onto SCGal-Ura and SCD-Ura plates for incubation at 30°C. Gal, galactose. (D) Wild-type cells, transformed with an empty vector or 2 μ vector bearing Hos3 driven under a galactose-inducible promoter, were first switched to galactose-containing medium, followed by cell cycle arrest with α-factor. Cells were then released into fresh medium and scored for anaphase cells at 15-min intervals (time points of 45, 60, 75, 90, and 105 min). (E) Wild-type cells, transformed with an empty vector or 2 μ vectors bearing Hos3 and Hos3H196E,D231N both driven under a galactose-inducible promoter, were analyzed as in C. (F) *hos3Δ* cells, transformed with an empty vector or 2 μ vectors bearing Bub2, Bfa1, and Kin4 all driven under a galactose-inducible promoter, were analyzed as in C. (G) *bub2Δ*, *bfa1Δ*, and *kin4Δ* cells, transformed with an empty vector or 2 μ vector bearing Hos3 driven under a galactose-inducible promoter, were analyzed as in C.

lethality (Ro *et al.*, 2002; D'Aquino *et al.*, 2005). Similarly, cells expressing high levels of Hos3 have significantly reduced cellular fitness and the association of Hos3 with both SPBs (Figure 7C). This property is likely due to an apparent delay in mitotic exit (Figure 7D) and is critically dependent on the lysine deacetylase activity of Hos3, as overexpression of HDAC-dead Hos3$^{H196E, D231N}$ does not inhibit growth (Figure 7E). Taken together, these data suggest that Hos3 functions as a SPOC component.

Given the remarkable similarity of phenotypic behavior between Hos3 and the known SPOC components, we further investigated their interdependence. Overexpression of the known SPOC components does not rescue the growth defect observed in the absence of Hos3 (Figure 7, F, compared with C). This is expected, since if Hos3 was required for loading the known SPOC components onto both SPBs, *hos3*Δ cells would display a severe rather than a partial SPOC defect, and the data in Figure 7A indicate that this is not the case. On the other hand, the reduced fitness by the overexpression of Hos3 is not affected by the absence of the known SPOC components (Figure 7, G, compared with C). This may suggest that the involvement of Hos3 in the SPOC is independent of these established components. Together the data argue for a novel SPOC role of Hos3 acting by a still largely unknown mechanism that could be in parallel with rather than dependent on the known Bub2/Bfa1/Kin4 pathway.

DISCUSSION

Role of Hos3 neck targeting for its SPB function

Our data establish that Hos3 displays a localization that is highly distinctive among known lysine deacetylases and tightly regulated in coordination with the cell cycle. In normally dividing yeast cells, Hos3 is a neck- and daughter SPB–localized protein. In such cells, the plane of cell division is defined by the bud neck, and the old SPB is inherited by the daughter cell, whereas the newly created SPB remains in the mother cell. The daughter SPB must traverse the plane circumscribed by the septin neck ring to establish the correct axis of spindle orientation. Once the correct spindle axis has been established, the daughter SPB acquires Hos3, and cells exit mitosis. In cells with impaired nuclear positioning such as *dyn1*Δ mutants, cells invoke a cell cycle delay and fail to exit mitosis until the spindle is correctly aligned. In this situation, we show that Hos3 is now recruited onto both SPBs and, of importance, that the prior association of Hos3 with the neck is necessary for this response to spindle misalignment.

Hos3 functions as SPOC component

A key feature shared among SPOC components is that they display cell cycle–dependent and asymmetric association with the SPB in unperturbed anaphase cells but are recruited simultaneously onto both SPBs in response to spindle misalignment. For example, the Bub2-Bfa1 complex, like Hos3, is only seen on the daughter SPB, whereas Kin4 transiently localizes to the mother SPB (Pereira *et al.*, 2000; Pereira and Schiebel, 2005; this study). The fact that Hos3 shares these key SPOC features prompted us to ask whether Hos3 is also a member of the SPOC. Two additional experiments suggest that Hos3 does indeed function as a SPOC component. First, the presence of Hos3 is necessary for the operation of the SPOC. In *hos3*Δ mutants, cells with a misaligned spindle were defective in mitotic arrest in a manner similar to the deletion of known SPOC component members (Figure 7A). Second, overexpression of Hos3 caused significantly reduced cellular fitness due to an apparent delay of mitotic exit (Figure 7, C and D). This physiological response is also observed when other SPOC components are constitutively overexpressed even in the presence of a normally aligned spindle.

How is Hos3 recruited to the bud neck?

Our results suggest that the Hos3 association with the neck is under the control of the morphogenesis checkpoint. The morphogenesis checkpoint is controlled by a series of hierarchical signaling events coordinated with cell cycle progression (reviewed in Howell and Lew, 2012). During our initial screening to identify mutants defective in Hos3 neck localization, we discovered that Hos3 remains cytosolic in mutants that fail to grow a bud, either via defects in bud site selection or polarization of Cdc42 (Supplemental Table S1). After budding, the septin ring is required for Hos3 neck localization, consistent with the role of septins as scaffolds for the recruitment of many bud neck–associated proteins. Addition of latrunculin B or nocodazole had no effect on the Hos3 neck pattern. This could be explained by the discovery that the downstream outputs of Cdc42 are largely independent of each other (Howell and Lew, 2012).

We propose the following sequence of events for the association of Hos3 to the bud neck: 1) Septins provide the initial scaffold to recruit several downstream proteins such as the Swe1 regulator kinases (Keaton and Lew, 2006); 2) Elm1 and Gin4 are essential to target and activate Hsl1 at the daughter side of the neck; 3) Hsl1 interacts with Hsl7; and 4) Hos3 is recruited to the neck via a direct interaction with Hsl7.

Although the morphogenesis checkpoint regulates Hos3 neck targeting, Hos3 is not a component of this checkpoint that regulates mitotic CDK activity (Supplemental Figure S7, C and D). This raises the question of why the cell uses the morphogenesis checkpoint to recruit Hos3 to the bud neck. One suggestion may be that such targeting machinery allows Hos3 to establish its SPOC response capability only at the appropriate phase of the cell cycle. Anaphase spindle elongation and orientation are monitored before mitotic exit but after mitotic entry. Therefore the SPOC functions between these two critical cell cycle landmarks. Because the morphogenesis checkpoint regulates mitotic entry, a neck-localized, Hsl7-dependent targeting of Hos3 guarantees Hos3 neck association only after the cell successfully enters the mitosis. Thus, after being targeted to the neck by Hsl1, Hsl7 likely plays two parallel functions: 1) to direct Swe1 for degradation and 2) to recruit Hos3 to the bud neck so that Hos3 is ready to function in the SPOC. In this manner, the involvement of the morphogenesis checkpoint allows Hos3 neck targeting only after appropriate mitotic entry, and from this moment on until mitotic exit, neck-localized Hos3 monitors spindle orientation as a component of the SPOC.

A second rationale for cells to make use of the morphogenesis checkpoint to recruit Hos3 to the bud neck would be that such targeting machinery directs Hos3 to a spatially appropriate cellular site for monitoring spindle orientation. Given that the Hsl1-Hsl7 module is asymmetrically neck associated, the asymmetry of Hsl7 explains the asymmetry of Hos3. The bud neck, where Hos3 is targeted, serves as a critical landmark for spindle alignment (Castillon *et al.*, 2003). A mother-bud axis exists upon polarity establishment until cytokinesis. As the cells go through anaphase, the spindle elongates, and the cytoplasmic microtubules pull the daughter SPB toward the daughter cell. Once this machinery moves the daughter SPB through the bud neck and into the nascent daughter cell, a correct spindle orientation is achieved. In contrast, a spindle orientation defect occurs if there are defects in the microtubule-dependent dynein pathway and the daughter SPB does not pass through the bud neck remaining within the mother cell. Hos3 appears to piggyback on the

morphogenesis checkpoint in order to be targeted to a convenient site for monitoring spindle orientation.

Cross-talk between the morphogenesis checkpoint and the SPOC?

The appropriate temporal regulation of the cell cycle guarantees correct division and inheritance between dividing cells. After DNA replication and cellular growth, when to enter and subsequently when to exit mitosis are key decisions for cells. The morphogenesis checkpoint regulates mitotic entry by modulating mitotic CDK activity. A variety of different physiological signals affect the operation of the morphogenesis checkpoint. In the presence of conditions that delayed daughter cell formation, cells spend longer in G2 of the cell cycle through the action of the morphogenesis checkpoint to allow mitotic entry only after cells readapt and grow a bud. In this manner, the morphogenesis checkpoint ensures that nuclear division happens only after budding.

After budding and nuclear replication, the two nuclei need to be separated parallel to the mother-bud axis to segregate correctly between the mother and daughter cells. This process of spindle positioning is dependent on the microtubule-dynein pathway and is monitored by the SPOC. On correct spindle elongation and positioning, the MEN activates mitotic exit. The SPOC monitors this status by inhibiting the MEN in case of spindle misorientation, ensuring that cells only exit mitosis after the spindle is correctly elongated and aligned.

Given its unique localization features in response to the action of morphogenesis checkpoint components and action in response to spindle misalignment, one speculative suggestion is that Hos3 may directly facilitate cross-talk between mitotic entry and exit, between the morphogenesis checkpoint and the SPOC. There is a precedent for such cross-talk. Elm1, the morphogenesis checkpoint member localized to the bud neck, facilitates the activation of the SPOC kinase Kin4 (Caydasi *et al.*, 2010b; Moore *et al.*, 2010). This suggests that the SPOC will be ready only after the morphogenesis checkpoint allows mitotic entry. Both Elm1 and Hos3 are recruited to the bud neck under the control of the morphogenesis checkpoint. Elm is itself a morphogenesis checkpoint member but not a SPOC member, and Hos3 is a SPOC component but not a member of the morphogenesis checkpoint. The benefit of this is the coordination of two checkpoints to facilitate an overall progression of consecutive events during the cell cycle.

Regulation of the SPOC components through targeting onto SPBs

A model for selective Hos3 targeting onto the SPBs might also apply to Bub2 and Bfa1, which display similar SPB-association features. The mechanism(s) by which Bub2 and Bfa1 are selectively loaded onto the daughter SPB in normal cells are unknown. Electron micrographs show that both Bub2 and Bfa1 are deposited onto the cytoplasmic side of the SPB (Daum *et al.*, 2000). Given the cytoplasmic localization of Hos3, it is reasonable to assume that the same applies to Hos3. We favor a model in which an unknown outer-plaque SPB component physically recruits Hos3 to the SPB and this component is associated with both SPBs, as Hos3 can potentially associate with both SPBs. This raises the question of how Hos3 is selectively loaded onto the daughter SPB in normal cells. One can envisage two alternative scenarios. Either there is an inhibitory zone exclusively within the mother cell to inhibit the interaction between Hos3 and the SPB, thus preventing Hos3 loading when the SPBs are still in the mother cell, or, alternatively, there is an activation zone within the daughter cell that drives Hos3 to associate with the daughter SPB. Our data show that in cells containing a misaligned spindle, both SPBs can be loaded with Hos3. We know that the NH2-terminus is required for the asymmetric Hos3 response. When this region is deleted, Hos3(*NΔ*) constitutively associates with the SPBs. These data suggest that the model of a "mother-cell-bound inhibitory zone" establishing an asymmetric pattern of SPB is the most parsimonious model. Because the cytosol is shared between the mother and emerging daughter cells, one possible mechanism to establish such an inhibitory zone is via proteins localized only to the mother cell cortex. Of interest, the SPOC component Kin4 localizes to the mother cell cortex throughout the cell cycle and was proposed to establish a mother-cell-restricted inhibitory zone for the MEN (Chan and Amon, 2009). In the presence of spindle misorientation, in addition to the SPOC response, the Kin4-based inhibitory zone further prevents MEN activation by excluding Tem1 from binding to both SPBs within the mother cell. In anaphase cells with normal spindles, Tem1 is loaded onto the daughter SPB to be activated, as the daughter cell is devoid of the Kin4-based inhibitory zone (Chan and Amon, 2009). Our proposed inhibitory zone for Hos3 would be analogous to the Kin4 inhibitory zone for Tem1 but differs in critical aspects. Hos3 is a SPOC component, but Tem1 is a MEN member. Therefore they have contradictory functions in promoting mitotic exit. Moreover, if Kin4 is responsible for establishment of a Hos3 inhibitory zone, Hos3 should be loaded constitutively and symmetrically onto the SPBs in *kin4Δ* cells, but this is not the case (unpublished data).

A key question for future studies is the identity of the unknown SPB component that recruits Hos3. A large-scale physical interaction screen identified an association between Hos3 and a SPB component, Cdc31 (Krogan *et al.*, 2006). Cdc31 is a potential candidate as the SPB recruiter for Hos3, but it remains to be established whether this interaction is direct.

Expansive view of lysine deacetylases

Finally, does our discovery of the novel function of Hos3 indicate a broader view of lysine deacetylases? We showed that the KDAC activity is not required for Hos3 localization (Supplemental Figure S3E) but is essential for its SPOC response. KDAC-dead Hos3H196E,D231N is unable to efficiently arrest anaphase cells with misaligned spindle (Figure 7B), nor could it inhibit the fitness of wild-type cells when overexpressed and associated with both SPBs (Figure 7E). These results lead to a novel role of reversible lysine acetylation in the regulation of mitosis.

Could KDACs play similar roles in other organisms? Members of the morphogenesis checkpoint and the SPOC have similar players in other organisms (e.g., Hsl7 as the homologue of human PRMT5; Bub2/Bfa1 as the homologue of fission yeast Cdc16/Byr4; Li, 1999; Lee *et al.*, 2000). However, the mechanism by which these entities regulate asymmetric cell division and its applicability to higher eukaryotes is largely an open question. Both budding yeast and mammals use a microtubule-based mobility system as a driving force to separate SPBs/centrosomes (Pereira and Yamashita, 2011). Of even more interest, the two SPBs in budding yeast and the two centrosomes in multicellular organisms display similar features of specified asymmetry. In budding yeast, the mother cell retains the newly duplicated SPB, whereas the daughter cell inherits the old SPB (Pereira *et al.*, 2001; Hotz *et al.*, 2012). In *Drosophila* male germline stem cells, the differentiating cell retains the daughter centrosome, whereas the mother centrosome is inherited by the cell that retains stem cell identity (Yamashita *et al.*, 2007).

Given the highly conserved regulation of spindle orientation, if the spindle is not correctly aligned with respect to the polarity-determining factors and mitosis persists, the outcome in budding

yeast will be a binucleate mother cell and an anucleate daughter cell. A similar situation for a mammalian cell results in aneuploidy, which drastically induces genomic instability and is a hallmark of systemic diseases such as cancer (Sen, 2000; Rajagopalan and Lengauer, 2004; Pellman, 2007; Sheltzer *et al*., 2011). These considerations suggest the existence of a mechanism functionally equivalent to the SPOC in the budding yeast that acts as a surveillance checkpoint to monitor spindle orientation in multicellular organisms. Indeed, a similar checkpoint named the centrosome orientation checkpoint (COC) has been found in *Drosophila* and activates a mitotic delay if the centrosomes are not properly oriented (Cheng *et al*., 2008). The interesting difference between the SPOC and the COC is that in budding yeast, the cell cycle is arrested by the SPOC before mitotic exit, but in *Drosophila* it is arrested by the COC before commitment to mitosis, which is the point of the cell cycle monitored by the morphogenesis checkpoint in budding yeast. It is intriguing to consider whether higher organisms have adopted and perhaps evolutionarily adapted a checkpoint that incorporates both the morphogenesis checkpoint and the SPOC to monitor spindle orientation to generate a reproducible and predictable outcome to an asymmetric cell division. It is even more intriguing to speculate on whether such checkpoints in higher organisms use lysine deacetylase enzymes in a manner similar to our observations of Hos3 in budding yeast.

MATERIALS AND METHODS

Yeast strains and plasmids

All yeast strains and plasmids used in this study are listed in Supplemental Tables S2 and S3, respectively. Strains are of S288C background unless otherwise indicated. Cells with constructs integrated at the genomic locus were grown to mid–log phase ($OD_{600} \approx 0.6$) in yeast/peptone/dextrose (YPD) medium; cells transformed with respective constructs were grown to mid–log phase ($OD_{600} \approx 0.6$) in synthetic complete dropout media. Double mutants or double genomically tagged strains were created by selecting the appropriate spore after sporulating the diploid cross between the two single mutants or genomically tagged strains.

Microscopy

Fluorescence and differential interference contrast (DIC) microscopy were performed using an Eclipse E600 microscope (Nikon, Tokyo, Japan). Cells expressing GFP or RFP fusion constructs were grown to mid–log phase in synthetic minimal medium and live imaged through fluorescein isothiocyanate or rhodamine filters. A series of *z*-stacks (1.6–3 μm in total depth with a 0.2-μm step for each section) were imaged by IPLab (Scanalytics, Milwaukee, WI). Raw data were deconvolved and analyzed by AutoQuant X software (Media Cybernetics, Rockville, MD). Fluorescence images shown are maximum projections of three-dimensional images.

Immunoblotting and immunoprecipitation

Genomically tagged cells were grown to mid–log phase ($OD_{600} \approx 0.6$) in YPD medium; cells transformed with respective constructs were grown to mid–log phase ($OD_{600} \approx 0.6$) in synthetic complete dropout (SCD) media. For immunoblotting, equal amounts of cells (a total of 10 OD_{600}) were collected by centrifugation and resuspended in TAz buffer (10 mM Tris, 10 mM sodium azide, pH 7.5) together with protease inhibitors (1 mM EDTA, 1 mM phenylmethylsulfonyl fluoride, 1 mM benzamidine, and 1 μg/ml pepstatin A). Cells were then subjected to multiple rounds (three to five ×1 min) of glass bead beating and checked for effective lysis under the microscope (>90% of cells were lysed). After spinning down the total cellular lysates, the supernatant was analyzed by SDS–PAGE and electrophoretically transferred onto nitrocellulose membrane (Pall Corp.). The membranes were blocked with 5% defatted milk in TBST (10 mM Tris, pH 7.5, 150 mM sodium chloride, and 0.1% Tween-20), and probed at room temperature with respective primary antibodies in TBST for 1 h and secondary antibodies in TBST for 30 min. Proteins of interest were detected through horseradish peroxidase (HRP) activity with an ECL kit (Pierce, Rockford, IL). For immunoprecipitation, cells were lysed by bead beating in phosphate-buffered saline (PBS) buffer (137 mM sodium chloride, 2.7 mM potassium chloride, 10 mM sodium phosphate dibasic, 2 mM potassium phosphate monobasic, 0.1% Triton X-100, pH 7.4) together with protease inhibitors (1 mM EDTA, 1 mM phenylmethylsulfonyl fluoride, 1 mM benzamidine, and 1 μg/ml pepstatin A). The total cellular lysates were clarified by centrifugation, and the supernatant was prepared for incubation with 30 μl prewashed anti-hemagglutinin (HA) agarose resin (Invitrogen, Carlsbad, CA) at 4°C for 4 h with gentle rocking. The resins were then washed three times in 1 ml of PBS buffer and eluted with SDS–PAGE sample buffer. After centrifugation of the resin, the supernatant was analyzed by immunoblotting for the detection of respective proteins. Antibodies used for this study were α-HA (32-6700; Invitrogen), α-Myc (SC-40; Santa Cruz Biotechnology, Dallas, TX), α-Clb2 (SC-9071; Santa Cruz Biotechnology), and α-tubulin (9280-0050G; AbD Serotec, Raleigh, NC).

Flow cytometry

Cells were grown to mid–log phase ($OD_{600} \approx 0.6$) in YPD medium. Equal numbers of cells (a total of ~0.8 OD_{600}) were collected by centrifugation and fixed with 70% ethanol at 4°C for ~12–14 h. Fixed cells were resuspended in 50 mM sodium citrate buffer (pH 7.4), sonicated for 15 s (50% cycle; Fisher Scientific Sonic Dismembrator) at setting 30%, and incubated with 0.5 mg/ml RNase at 50°C for 1 h, followed by 1 mg/ml proteinase K at 50°C for 1 h. After being spun down, cells were resuspended in 50 mM sodium citrate buffer (pH 7.4) and stained with 16 μg/ml propidium iodide in the dark at room temperature for 30 min. Finally, cells were subjected to analysis by an LSR II flow cytometer (Becton Dickinson, Franklin Lakes, NJ)

ACKNOWLEDGMENTS

We thank Mark Longtine, Marc R. Gartenberg, Troy Harkness, and Scott Emr for strains and plasmids used in this study; Chris Stefan for assistance with time-lapse fluorescence microscopy; and Lavanya Sayam for help with flow cytometry. This work was supported by a grant from the National Institutes of Health (5R01GM069596) to R.N.C.

REFERENCES

Ahn S-H, Diaz RL, Grunstein M, Allis CD (2006). Histone H2B deacetylation at lysine 11 is required for yeast apoptosis induced by phosphorylation of H2B at serine 10. Mol Cell 24, 211–220.

Akella JS, Wloga D, Kim J, Starostina NG, Lyons-Abbott S, Morrissette NS, Dougan ST, Kipreos ET, Gaertig J (2010). MEC-17 is an alpha-tubulin acetyltransferase. Nature 467, 218–222.

Babour A, Bicknell AA, Tourtellotte J, Niwa M (2010). A surveillance pathway monitors the fitness of the endoplasmic reticulum to control its inheritance. Cell 142, 256–269.

Bardin AJ, Amon A (2001). MEN and SIN: what's the difference? Nat Rev. Mol Cell Biol 2, 815–826.

Barral Y, Parra M, Bidlingmaier S, Snyder M (1999). Nim1-related kinases coordinate cell cycle progression with the organization of the peripheral cytoskeleton in yeast. Genes Dev 13, 176–187.

Bjerling P, Silverstein RA, Thon G, Caudy A, Grewal S, Ekwall K (2002). Functional divergence between histone deacetylases in fission yeast

by distinct cellular localization and in vivo specificity. Mol Cell Biol 22, 2170–2181.
Blacketer MJ, Koehler CM, Coats SG, Myers AM, Madaule P (1993). Regulation of dimorphism in *Saccharomyces cerevisiae*: involvement of the novel protein kinase homolog Elm1p and protein phosphatase 2A. Mol Cell Biol 13, 5567–5581.
Carmen AA, Griffin PR, Calaycay JR, Rundlett SE, Suka Y, Grunstein M (1999). Yeast HOS3 forms a novel trichostatin A-insensitive homodimer with intrinsic histone deacetylase activity. Proc Natl Acad Sci USA 96, 12356–12361.
Castillon GA, Adames NR, Rosello CH, Seidel HS, Longtine MS, Cooper JA, Heil-Chapdelaine RA (2003). Septins have a dual role in controlling mitotic exit in budding yeast. Curr Biol 13, 654–658.
Caydasi A, Ibrahim B, Pereira G (2010a). Monitoring spindle orientation: spindle position checkpoint in charge. Cell Division 5, 28.
Caydasi AK, Kurtulmus B, Orrico MI, Hofmann A, Ibrahim B, Pereira G (2010b). Elm1 kinase activates the spindle position checkpoint kinase Kin4. J Cell Biol 190, 975–989.
Chan LY, Amon A (2009). The protein phosphatase 2A functions in the spindle position checkpoint by regulating the checkpoint kinase Kin4. Genes Dev 23, 1639–1649.
Cheng J, Turkel N, Hemati N, Fuller MT, Hunt AJ, Yamashita YM (2008). Centrosome misorientation reduces stem cell division during ageing. Nature 456, 599–604.
Choudhary C, Kumar C, Gnad F, Nielsen ML, Rehman M, Walther TC, Olsen JV, Mann M (2009). Lysine acetylation targets protein complexes and co-regulates major cellular functions. Science 325, 834–840.
Chou C-C, Li Y-C, Gartenberg MR (2008). Bypassing Sir2 and O-acetyl-ADP-ribose in transcriptional silencing. Mol Cell 31, 650–659.
Cid VJ, Jiménez J, Molina M, S M, Nombela C, Thorner JW (2002). Orchestrating the cell cycle in yeast: sequential localization of key mitotic regulators at the spindle pole and the bud neck. Microbiology 148, 2647–2659.
Cid VJ, Shulewitz MJ, McDonald KL, Thorner J (2001). Dynamic localization of the Swe1 regulator Hsl7 during the *Saccharomyces cerevisiae* cell cycle. Mol Biol Cell 12, 1645–1669.
Conacci-Sorrell M, Ngouenet C, Eisenman RN (2010). Myc-Nick: a cytoplasmic cleavage product of Myc that promotes alpha-tubulin acetylation and cell differentiation. Cell 142, 480–493.
D'Aquino KE, Monje-Casas F, Paulson J, Reiser V, Charles GM, Lai L, Shokat KM, Amon A (2005). The protein kinase Kin4 inhibits exit from mitosis in response to spindle position defects. Mol Cell 19, 223–234.
Daum JR, Gomez-Ospina N, Winey M, Burke DJ (2000). The spindle checkpoint of *Saccharomyces cerevisiae* responds to separable microtubule-dependent events. Curr Biol 10, 1375–1378.
Drees BL, Sundin B, Brazeau E, Caviston JP, Chen GC, Guo W, Kozminski KG, Lau MW, Moskow JJ, Tong A, *et al*. (2001). A protein interaction map for cell polarity development. J Cell Biol 154, 549–571.
Ekwall K (2005). Genome-wide analysis of HDAC function. Trends Genet 21, 608–615.
Finnin MS, Donigian JR, Cohen A, Richon VM, Rifkind RA, Marks PA, Breslow R, Pavletich NP (1999). Structures of a histone deacetylase homologue bound to the TSA and SAHA inhibitors. Nature 401, 188–193.
Gu W, Roeder RG (1997). Activation of p53 sequence-specific DNA binding by acetylation of the p53 C-terminal domain. Cell 90, 595–606.
Heil-Chapdelaine RA, Oberle JR, Cooper JA (2000). The cortical protein Num1p is essential for dynein-dependent interactions of microtubules with the cortex. J Cell Biol 151, 1337–1344.
Holt LJ, Tuch BB, Villén J, Johnson AD, Gygi SP, Morgan DO (2009). Global analysis of Cdk1 substrate phosphorylation sites provides insights into evolution. Science 325, 1682–1686.
Hotz M, Leisner C, Chen D, Manatschal C, Wegleiter T, Ouellet J, Lindstrom D, Gottschling DE, Vogel J, Barral Y (2012). Spindle pole bodies exploit the mitotic exit network in metaphase to drive their age-dependent segregation. Cell 148, 958–972.
Howell AS, Lew DJ (2012). Morphogenesis and the cell cycle. Genetics 190, 51–77.
Hubbert C, Guardiola A, Shao R, Kawaguchi Y, Ito A, Nixon A, Yoshida M, Wang X-F, Yao T-P (2002). HDAC6 is a microtubule-associated deacetylase. Nature 417, 455–458.
Janke C, Bulinski JC (2011). Post-translational regulation of the microtubule cytoskeleton: mechanisms and functions. Nat Rev Mol Cell Biol 12, 773–786.
Jaspersen SL, Winey M (2004). The budding yeast spindle pole body: structure, duplication, and function. Annu Rev Cell Dev Biol 20, 1–28.
Kawaguchi Y, Kovacs JJ, McLaurin A, Vance JM, Ito A, Yao T-P (2003). The deacetylase HDAC6 regulates aggresome formation and cell viability in response to misfolded protein stress. Cell 115, 727–738.
Keaton MA, Lew DJ (2006). Eavesdropping on the cytoskeleton: progress and controversy in the yeast morphogenesis checkpoint. Curr Opin Microbiol 9, 540–546.
Keogh M-C, Kurdistani SK, Morris SA, Ahn SH, Podolny V, Collins SR, Schuldiner M, Chin K, Punna T, Thompson NJ, *et al*. (2005). Cotranscriptional Set2 methylation of histone H3 lysine 36 recruits a repressive Rpd3 complex. Cell 123, 593–605.
Kim SC, Sprung R, Chen Y, Xu Y, Ball H, Pei J, Cheng T, Kho Y, Xiao H, Xiao L, *et al*. (2006). Substrate and functional diversity of lysine acetylation revealed by a proteomics survey. Mol Cell 23, 607–618.
Kozubowski L, Larson JR, Tatchell K (2005). Role of the septin ring in the asymmetric localization of proteins at the mother-bud neck in *Saccharomyces cerevisiae*. Mol Biol Cell 16, 3455–3466.
Krogan NJ, Cagney G, Yu H, Zhong G, Guo X, Ignatchenko A, Li J, Pu S, Datta N, Tikuisis AP, *et al*. (2006). Global landscape of protein complexes in the yeast *Saccharomyces cerevisiae*. Nature 440, 637–643.
Lee JH, Cook JR, Pollack BP, Kinzy TG, Norris D, Pestka S (2000). Hsl7p, the yeast homologue of human JBP1, is a protein methyltransferase. Biochem Biophys Res Commun 274, 105–111.
Lew DJ (2000). Cell-cycle checkpoints that ensure coordination between nuclear and cytoplasmic events in *Saccharomyces cerevisiae*. Curr Opin Genet Dev 10, 47–53.
Lew DJ, Burke DJ (2003). The spindle assembly and spindle position checkpoints. Annu Rev Genetics 37, 251–282.
Li R (1999). Bifurcation of the mitotic checkpoint pathway in budding yeast. Proc Natl Acad Sci USA 96, 4989–4994.
Li YY, Yeh E, Hays T, Bloom K (1993). Disruption of mitotic spindle orientation in a yeast dynein mutant. Proc Natl Acad Sci USA 90, 10096–10100.
Lin S-J, Defossez P-A, Guarente L (2000). Requirement of NAD and SIR2 for life-span extension by calorie restriction in *Saccharomyces cerevisiae*. Science 289, 2126–2128.
Longtine MS, Fares H, Pringle JR (1998). Role of the yeast Gin4p protein kinase in septin assembly and the relationship between septin assembly and septin function. J Cell Biol 143, 719–736.
Luo J, Su F, Chen D, Shiloh A, Gu W (2000). Deacetylation of p53 modulates its effect on cell growth and apoptosis. Nature 408, 377–381.
Maekawa H, Priest C, Lechner J, Pereira G, Schiebel E (2007). The yeast centrosome translates the positional information of the anaphase spindle into a cell cycle signal. J Cell Biol 179, 423–436.
Markus SM, Lee W (2011). Microtubule-dependent path to the cell cortex for cytoplasmic dyneien in mitotic spindle orientation. BioArchitecture 1, 209–215.
McMillan JN, Longtine MS, Sia RA, Theesfeld CL, Bardes ES, Pringle JR, Lew DJ (1999). The morphogenesis checkpoint in *Saccharomyces cerevisiae*: cell cycle control of Swe1p degradation by Hsl1p and Hsl7p. Mol Cell Biol 19, 6929–6939.
Moore JK, Chudalayandi P, Heil-Chapdelaine RA, Cooper JA (2010). The spindle position checkpoint is coordinated by the Elm1 kinase. J Cell Biol 191, 493–503.
Oh Y, Bi E (2011). Septin structure and function in yeast and beyond. Trends Cell Biol 21, 141–148.
Pellman D (2007). Cell biology: aneuploidy and cancer. Nature 446, 38–39.
Pereira G, Höfken T, Grindlay J, Manson C, Schiebel E (2000). The Bub2p spindle checkpoint links nuclear migration with mitotic exit. Mol Cell 6, 1–10.
Pereira G, Schiebel E (2005). Kin4 kinase delays mitotic exit in response to spindle alignment defects. Mol Cell 19, 209–221.
Pereira G, Tanaka TU, Nasmyth K, Schiebel E (2001). Modes of spindle pole body inheritance and segregation of the Bfa1p-Bub2p checkpoint protein complex. EMBO J 20, 6359–6370.
Pereira G, Yamashita YM (2011). Fly meets yeast: checking the correct orientation of cell division. Trends Cell Biol 21, 526–533.
Rajagopalan H, Lengauer C (2004). Aneuploidy and cancer. Nature 432, 338–341.
Ro H-S, Song S, Lee KS (2002). Bfa1 can regulate Tem1 function independently of Bub2 in the mitotic exit network of *Saccharomyces cerevisiae*. Proc Natl Acad Sci USA 99, 5436–5441.
Robert T, Vanoli F, Chiolo I, Shubassi G, Bernstein KA, Rothstein R, Botrugno OA, Parazzoli D, Oldani A, Minucci S, *et al*. (2011). HDACs link the DNA damage response, processing of double-strand breaks and autophagy. Nature 471, 74–79.

Robyr D, Suka Y, Xenarios I, Kurdistani SK, Wang A, Suka N, Grunstein M (2002). Microarray deacetylation maps determine genome-wide functions for yeast histone deacetylases. Cell 109, 437–446.

Rusche LN, Kirchmaier AL, Rine J (2003). The establishment, inheritance, and function of silenced chromatin in *Saccharomyces cerevisiae*. Annu Rev Biochem 72, 481–516.

Sen S (2000). Aneuploidy and cancer. Curr Opin Oncol 12, 82–88.

Shahbazian MD, Grunstein M (2007). Functions of site-specific histone acetylation and deacetylation. Annu Rev Biochem 76, 75–100.

Sheltzer JM, Blank HM, Pfau SJ, Tange Y, George BM, Humpton TJ, Brito IL, Hiraoka Y, Niwa O, Amon A (2011). Aneuploidy drives genomic instability in yeast. Science 333, 1026–1030.

Shida T, Cueva JG, Xu Z, Goodman MB, Nachury MV (2010). The major alpha-tubulin K40 acetyltransferase alphaTAT1 promotes rapid ciliogenesis and efficient mechanosensation. Proc Natl Acad Sci USA 107, 21517–21522.

Shulewitz MJ, Inouye CJ, Thorner J (1999). Hsl7 localizes to a septin ring and serves as an adapter in a regulatory pathway that relieves tyrosine phosphorylation of Cdc28 protein kinase in *Saccharomyces cerevisiae*. Mol Cell Biol 19, 7123–7137.

Theesfeld CL, Zyla TR, Bardes EGS, Lew DJ (2003). A monitor for bud emergence in the yeast morphogenesis checkpoint. Mol Biol Cell 14, 3280–3291.

Turner EL, Malo ME, Pisclevich MG, Dash MD, Davies GF, Arnason TG, Harkness TAA (2010). The *Saccharomyces cerevisiae* anaphase-promoting complex interacts with multiple histone- modifying enzymes to regulate cell cycle progression. Eukaryot Cell 9, 1418–1431.

Versele M, Thorner J (2004). Septin collar formation in budding yeast requires GTP binding and direct phosphorylation by the PAK, Cla4. J Cell Biol 164, 701–715.

Walch-Solimena C, Collins RN, Novick PJ (1997). Sec2p mediates nucleotide exchange on Sec4p and is involved in polarized delivery of post-Golgi vesicles. J Cell Biol 137, 1495–1509.

Weinert BT, Wagner SA, Horn H, Henriksen P, Liu WR, Olsen JV, Jensen LJ, Choudhary C (2011). Proteome-wide mapping of the *Drosophila* acetylome demonstrates a high degree of conservation of lysine acetylation. Sci Signal 4, ra48.

Weiss EL, Bishop AC, Shokat KM, Drubin DG (2000). Chemical genetic analysis of the budding-yeast p21-activated kinase Cla4p. Nat Cell Biol 2, 677–685.

Yamashita YM, Mahowald AP, Perlin JR, Fuller MT (2007). Asymmetric inheritance of mother versus daughter centrosome in stem cell division. Science 315, 518–521.

Zhang X, Yuan Z, Zhang Y, Yong S, Salas-Burgos A, Koomen J, Olashaw N, Parsons JT, Yang X-J, Dent SR, *et al*. (2007). HDAC6 modulates cell motility by altering the acetylation level of cortactin. Mol Cell 27, 197–213.

Zhao S, Xu W, Jiang W, Yu W, Lin Y, Zhang T, Yao J, Zhou L, Zeng Y, Li H, *et al*. (2010). Regulation of cellular metabolism by protein lysine acetylation. Science 327, 1000–1004.